Phase equilibria in solutions of disklike particles

Maciej Wnek and Jozef K. Moscicki*
Institute of Physics, Jagiellonian University, 30-059 Krakow, Reymonta 4, Poland
(Received 13 January 1995)

The Flory lattice method has been utilized to study phase equilibria in solutions of disklike molecules. It is found that the critical disk diameter-to-width ratio x for the formation of the stable nematic phase is about 3.015. Temperature-concentration phase diagrams are studied for several values of x. For $x < 8.6$ the isotropic and nematic phases are separated by a biphasic range of concentrations. Above $x \approx 8.6$ a reentrant nematic feature appears, i.e., at a given temperature either of two pairs of phases, isotropic-nematic or nematic-nematic, occurred. The locations of the corresponding critical and triple points are computed.

PACS number(s): 61.30.Cz, 64.70.Md

I. INTRODUCTION

Given the prevalence of close packing at normal liquid densities and the short range of the intermolecular repulsion compared with the range of attractive intermolecular forces, it is commonly accepted that the spatial arrangement of molecules in liquids is dictated by their shapes rather than by forces of attraction [1–4]. Consequently, thermodynamic properties of liquids are frequently studied theoretically by first considering the configuration of a system of hard particles (characterized by a repulsive contact interaction), with other kinds of interactions introduced a later stage as perturbative effects [2–6]. In such a model, the configuration partition function usually reduces to the product of a combinatory factor and the Boltzmann exponential of the intermolecular energy, customarily represented by a mean field.

Flory and co-workers explored over the years such a model of liquid crystalline nematic and isotropic phases consisting of rigid and semirigid rodlike molecules either as the sole constituent of the neat liquid (thermotropics) or as a solute (lyotropics) [5–23]. Because of the particular shape of these molecules, they found a lattice method especially useful for evaluating the configuration partition function, especially the steric factor describing spatial configurations without molecular overlaps [5]. The lattice discretization of molecular orientations requires breaking the molecule up into a number of segments parallel and perpendicular to the preferred direction (the director) in the ordered phase. The disorder index of a molecule, y, is defined as the projection of the rod of axial ratio x in a plane normal to the director. In the model, the disorder index characterizes the degree of orientational order of the long molecular axes more naturally than the commonly used (nematic) order parameter S. As a result of the discretization procedure, the hard-rod fluid with continuously varying molecular orientations is then replaced by a fluid characterized by perfect orientational order but polydisperse length. Since the distribution of segments in any given row of the lattice cells parallel to the director is assumed random and uninfluenced by conditions in the neighboring rows, a nematic phase in the neat system of rodlike molecules is the only stable phase that is predicted above a critical axial ratio (the length-to-diameter ratio), the particular value of which depends on details of each model considered [5,11,14,24]. The formation of a translationally ordered phase, e.g., the smectic phase, would require the introduction of appropriate intermolecular interactions such as impenetrable boundaries [25]. For the Flory method, this program has yet to be accomplished.

It is well known that not only rodlike, but also disklike molecules exhibit liquid crystallinity at properly chosen conditions (e.g., temperature, pressure, or composition) [26–31]. Such systems are, however, much more difficult to study theoretically. While the thermodynamic behavior of rodlike particles has been studied for many years [4,5,12–19,32–35], relevant studies of discotic molecules have been less frequent [36–45].

Compared to rodlike systems, the lattice method is not as easy to implement for discotic systems because of the particular shape anisotropy of the disklike molecules. Only simplified versions of the original Flory approach, in particular, treatments in which the orientations of the disks are limited to the orthogonal axes of the usual cubic lattice, have been explored in modeling the phase behavior of discotic micelles in lyotropic solutions [36,46].

In this paper we report what is to our knowledge the first lattice treatment in which continuous variation of disk disorientation is allowed. We have carried out an approximate treatment of systems containing hard disks present either as a solute or as the sole constituent of the neat liquid. The complexity of the problem arises from the fact that in the case of disklike particles one has to accommodate on a lattice a particle which is quasi-two-dimensional. Due to the cylindrical symmetry of the disks and the axial symmetry of the nematic phase, the perfectly ordered disklike molecules are approximated by rectangular parallelepipeds of the breadth-to-width ratio x. Disorientation is described via two independent rotations about the **X** and **Y** laboratory frame axes, respectively. Consequently, two disorder indices are required. The degree of disorder is allowed to vary continuously, and the disks assume a distribution of disorientation dependent on x and the concentration. Initially, the only interaction accounted for is contact repulsion and the con-

*Electronic address: ufmoscic@cyf-kr.edu.pl

figurational partition function is evaluated. The theory predicts a threshold value of $x_{cr} \simeq 3.015$ for the formation of the nematic phase of the neat system of disks. The solvent-solute interaction energy is incorporated into the theory later.

As will become apparent later, there is a profound reciprocity between a number of approximations in this work and those used by Flory in the original version of the lattice model for rods [5]. We believe that this feature guarantees consistency in the lattice treatment of the nematic phase for both kinds of molecules, and thus is fundamental for future work which will construct a consistent Flory lattice method description of the phase equilibria of a solution of rodlike and disklike micelle mixtures, and of a solution of biaxial discotic particles, in particular the appearance of the biaxial nematic phase.

II. THEORY

The phase equilibrium theory developed here concerns a system of identical disks dispersed in a solvent. Following the case of rodlike particles, we stipulate that solutions of sufficiently asymmetric disks should exhibit phase separation and coexistence of a less concentrated isotropic phase of unoriented disks and a somewhat denser nematic phase consisting of partially oriented disks. The phase equilibrium between the isotropic (I) and nematic (N) phases requires the chemical potentials of the same component of the solution in both phases to be equal:

$$(\mu_i - \mu_i^0)^I = (\mu_i - \mu_i^0)^N \ , \tag{1}$$

where $i = s$ or x denotes solvent or solute, respectively. By definition, the chemical potentials are

$$\begin{aligned} \frac{\mu_i^N - \mu_i^0}{RT} &= \left(\frac{\partial G^N}{\partial n_i}\right)_{T,V,eq} = -\left(\frac{\partial \ln Z^N}{\partial n_i}\right)_{T,V,eq} , \\ \frac{\mu_i^I - \mu_i^0}{RT} &= \left(\frac{\partial G^I}{\partial n_i}\right)_{T,V} = -\left(\frac{\partial \ln Z^I}{\partial n_i}\right)_{T,V} , \end{aligned} \tag{2}$$

where G is the Gibbs free energy, R is the universal gas constant, Z is the partition function, and T and V denote the absolute temperature and sample volume, respectively. The subscript *"eq"* signifies the orientational equilibrium of disks in the nematic phase.

In general, the partition function Z is considered to be composed of three factors: the combinatory or steric factor Z_{comb}, the orientational factor Z_{or}, and the factor introducing the exchange free energies of interaction between the solvent and disks, Z_{int}:

$$Z = Z_{comb} Z_{or} Z_{int} \ . \tag{3}$$

In estimating the steric factor Z_{comb} our theory benefits from the original Flory method [5]. Adopting a customary simplification, we consider a solution consisting of n_s approximately isodiametric spherical solvent molecules and n_x rigid disklike molecules of the same thickness and x times as wide. The volume occupied by the solution is then subdivided into a cubic array of n_0 cells of linear dimension equal to the diameter of the solvent particle (and the disk thickness). We assume that each solvent molecule can only fully occupy a cell of the lattice. Similarly, each disk consists of contiguous fully occupied cells. Therefore $n_0 = n_s + x^2 n_x$. Let the nematic director be the lattice **Z** axis. Because of the disk's cylindrical symmetry and also the axial symmetry of its orientations about the director, the order of the long axes and disk rotations about the short axis are not germane to the present problem. A perfectly ordered disk of molecular volume v is sufficiently well approximated by $x \times x \times 1$: a *rectangular parallelepiped* with the long edges parallel to the **X** and **Y** lattice axes, cf. Fig. 1. In other words, the number of cells occupied by the disk, or its molecular volume, is

$$v = x^2 \ . \tag{4}$$

(Note that, contrary to the original Flory notation, x describes now the *flatness*, the diameter-to-width ratio of the real disklike molecule [5].)

We start from the perfectly ordered system, i.e., all the disks are parallel to the lattice reference plane **XY** and the disk normal is parallel to **Z**. Let us next introduce a small orientational disorder of the disks. All spatial orientations of a disk can be realized by a superposition of two independent, orthogonal *declinations* of the disk from the perfect order, (1) by an angle θ_x about the **X** axis of the lattice, and (2) by an angle θ_y about the **Y** axis of the lattice. Thus a disk rotated by a small θ_x is approximated on the lattice as a "stairway" made out of rods of length x, cf. Fig. 2.

The second rotation by θ_y inclines the stairway structure sideways, producing a secondary segmentation of the stairway steps, cf. Fig. 3.

Both declinations can be parametrized by their respective disorder indexes, y_X and y_Y. The disorder index y_I corresponds to rotation about either the I=**X** or **Y** axis and is defined as the ratio between the projection of the surface of the disk onto the I**Z** plane and x, cf. Fig. 3.

The overall disorder of the disk, y, we define as the arithmetic mean of the two:

$$y = \frac{(y_X + y_Y)}{2} \ . \tag{5}$$

Note that our definition of disorder, which is analogous to the disorder index introduced by Flory and

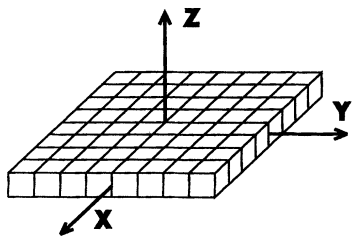

FIG. 1. Perfectly ordered model disk with $x = 8$.

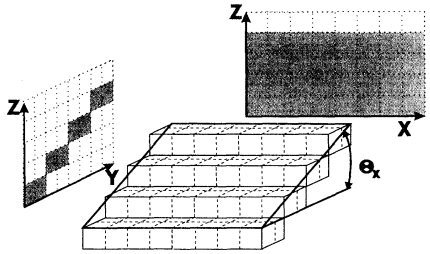

FIG. 2. Disk with $x = 8$ after rotation around the **X** axis by θ_x yelding the disorder index $y_X = 4$. Projections of the disk onto the **XZ** and **YZ** planes are also shown.

Ronca, affords the correct description of the relationship between y and the spatial orientation of the disklike molecule [14,47].

Thus for the perfectly ordered disk we have, cf. Fig. 1,

$$y_X = y_Y = y = 1 , \tag{6}$$

and for a phase with cylindrical symmetry we expect for the system in equilibrium

$$\bar{y}_X = \bar{y}_Y = \bar{y} , \tag{7}$$

where the bar denotes the ensemble average.

We note at this point that the assumption that disks with the same y are equivalent, although in accord with the Flory model philosophy, contains an inaccuracy which, for significant orientational disorder of disks, can be quite severe [14]. Because of the cylindrical symmetry of the nematic phase, the solid angle swept out by the end of a unit vector normal to a real discotic molecule assuming all possible equivalent molecular orientations is a cone about the director (about the **Z** axis), i.e., the declination angle is constant. For the lattice approximation considered here, however, because of the chosen definition of the declination angles (θ_x, θ_y) the solid angle is a pyramidal cone about the **Z** axis, i.e., the declination angle varies along the pyramid square base. Fortunately, for the small declinations which are of the greatest importance in the nematic phase, the discrepancy is of minor significance. For the isotropic phase, however, where by definition declinations are large, the problem needs careful consideration.

A. Nematic phase

1. *Combinatory or "steric" factor Z_{comb}*

Let us assume that j disks have already been assigned locations on the lattice. We estimate the number (ν_{j+1}) of sites available to an additional disk $j+1$, the orientation of which is specified by y_X and y_Y. The disk is divided into $(y_X + y_Y - 1)$ trains of contiguous subparticles (segments) located in neighboring elementary **XY** slices of the lattice (orthogonal to the director **Z**), cf. Figs. 3 and 4. In the spirit of the Flory approximation, we consider the trains to be independent of each other, their distribution in any given **XY** slice to be random, and uninfluenced by conditions in neighboring slices. Furthermore, due to the positional disorder of the nematic phase, the composition of each slice should be the same (no smectic order).

Thus the problem reduces to placing these new $(y_X + y_Y - 1)$ trains in **XY** slices, given that the slices are already populated by trains from the previously "dissolved" j disks. The justification for this model rests on the plausible assertion that the probability of vacancies throughout the designated set of x^2 lattice sites comprising $y_X y_Y$ segments should closely approximate the probability that a given cylindrical disklike volume chosen for occupation by a real disk inclined at the same angles (θ_x, θ_y) from the plane normal to the director is empty, taking the short-range order of the liquid into account in an appropriate way. The error should be negligible for small values of $\bar{y}/x$, but for highly disordered disks, e.g., in the isotropic phase, the approximation is less certain. We will address this point further in the following. In the highly ordered nematic phase, the approximation is excellent.

Due to the cylindrical symmetry of the system about the **Z** axis, the orientations of trains in the **XY** slices are uniformly distributed about the axis. Because of the phase symmetry, the **X** and **Y** axes are interchangeable, so that the particular orientation of the trains of disk $j+1$ should be of no importance for the final result. Let the **X** axis be the reference axis. Then the train orien-

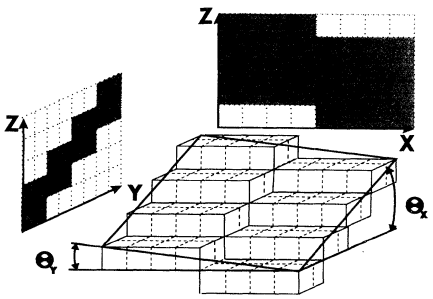

FIG. 3. The same disk after a second rotation around the **Y** axis by Θ_y, $y_Y = 2$.

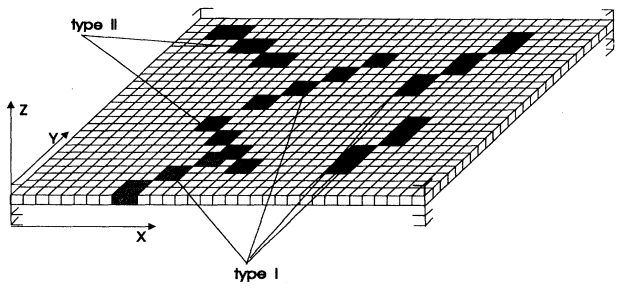

FIG. 4. **XY** slice of the lattice with trains (in black) oriented in the I, positive, and II, negative, sense. A failed attempt to place the shaded train is also shown.

tation in a slice can be either I positive or II negative with respect to the reference axis, cf. Fig. 4. For convenience let us assume that the orientation of the train under consideration is positive.

Due to the fact that the segment sides are always parallel to either the **X** or the **Y** axes, we may assume that only neighboring occupied segments reduce the probability that sites required for the next train segment are already occupied by other trains in the slice, cf. Fig. 4. For example, the influence of the first train segment on the conditional probability of finding free space for the third segment is negligible. Therefore we assume that the probability of finding vacant cells in the slice for every segment of the train is the same, P_2, except for the first, P_1. Consequently, all $y_X y_Y$ segments of the disk $j{+}1$ are either of the "first" ($y_X + y_Y - 1$ of them) or "other," second kind, and the number ν_{j+1} of sites available to the additional disk $j{+}1$ can be simply written as

$$\nu_{j+1} = n_0 \, P_1^{(y_X+y_Y-1)} \, P_2^{(y_X y_Y - y_X - y_Y + 1)} . \tag{8}$$

Our goal is thus reduced to calculating P_i, $i = 1$ (first) or 2 (other).

The segment assignment to a location on the cubic lattice was considered by Shih and Alben [36,46]. Using their approach, we implement a convenient algorithm for placing cells of the μth segment. Moving along the long axis of the train from the lower left-hand end onward we identify the cells as follows, cf. Fig. 5: the bottom corner cell (we will call them cells of type μa); the remaining cells of the left (μb) or of the right ($\mu b'$) side of the segment (with respect to the long axis), alternating the label cell by cell between b and b' to preserve the interchangeability of **X** and **Y** (and thus of y_X and y_Y) [46]. Finally, we identify the remaining cells of the segment, starting again from the bottom corner and labeling them (μc).

The segregation of cells into different types is not accidental; the probability of finding vacant sites for cells of a given type is not broadly distributed. We may then introduce the mean probability of finding a vacant site of a particular type which greatly simplifies subsequent developments. The probability of finding vacant cells for the μth segment will then be a product of the (mean) probabilities of finding vacant sites of type μa, μb, $\mu b'$, or μc, which we estimate in turn.

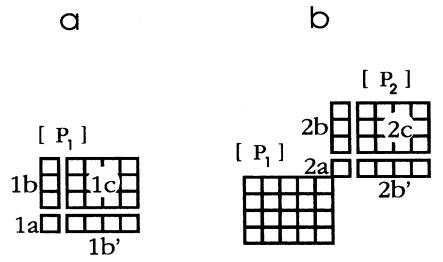

FIG. 5. Implemented segregation of (a) first (b) other segment cells into different types.

The probability that a given site is free for the $1a$ cell of the first ($\mu = 1$) segment, p_{1a}, is

$$p_{1a} = \frac{(n_0 - jx^2)}{n_0} . \tag{9}$$

The conditional probability that each succeeding site is vacant is given, in accord with the original Flory approach [5], by the mole fraction of vacant sites in a random distribution of segments and empty sites:

$$p_i = \frac{(n_0 - jx^2)}{n_0 - jx^2 + \sum_{\ell} K_i'(x, y_X^{\ell}, y_Y^{\ell})} , \tag{10}$$

where the subscript i denotes the kind of segment cell considered, ℓ numbers disks in the system, and the occupation factor $K_i'(x, y_X^{\ell}, y_Y^{\ell})$ is the number of ways the given site can be occupied by the ℓth disk.

If we are allowed to preserve the specified angular distribution of molecular symmetry axes throughout the process of addition of the solute molecules, the average $\bar{y}$ introduced in Eq. (7) remains fixed. Moreover, the geometric mean of K_i' over the distribution may be used; hence y_X^{ℓ} and y_Y^{ℓ} in Eq. (10) should also be replaced by their means. Given that the occupation factors turn out to be second order polynomials in y_X and y_Y (cf. the Appendix), and the following relations obtain:

$$\sum_j^{n_x} (y_X^j + y_Y^j) \equiv 2n_x\bar{y} \quad \text{and} \quad \sum_j^{n_x} (y_X^j y_Y^j) \cong n_x \bar{y}^2 , \tag{11}$$

the expression for p_i takes the form

$$p_i \simeq \frac{(n_0 - jx^2)}{n_0 - j[x^2 - K_i(x, \bar{y})]} , \tag{12}$$

where $K_i(x, \bar{y})$ is the average disk occupation factor, derived in the Appendix.

We remind the reader at this point that, since the p_i are conditional probabilities, evaluation of the $K_i(x, \bar{y})$ factors can only occur after the cells have been appropriately assigned, i.e., for a given i one assumes that all preceding cells of the train are already placed; for example, all $1a$, $1b$, $1b'$, $1c$, and $2a$ cells should already be placed before we calculate K_{2b} or $K_{2b'}$.

Because of the cylindrical symmetry of the system and the symmetries that exist between segments of the same train, some K_i factors are identical. In particular, one finds that the K_i factors should satisfy the following identities:

$$K_{1c}(x, \bar{y}) = K_{2c}(x, \bar{y}) \tag{13}$$

and

$$K_{nb}(x, \bar{y}) = K_{nb'}(x, \bar{y}), \quad n = 1, 2. \tag{14}$$

This allows further simplification of P_1 and P_2:

$$P_1 = p_{1a} \, p_{1b}^{(x/y_X + x/y_Y - 2)} \, p_{1c}^{(x/y_X - 1)(x/y_Y - 1)} , \tag{15}$$

$$P_2 = p_{2a} \, p_{2b}^{(x/y_X + x/y_Y - 2)} \, p_{1c}^{(x/y_X - 1)(x/y_Y - 1)} , \tag{16}$$

where each p_i has the form of Eq. (12) with the relevant K_i (cf. the Appendix)

$$K_{1b}(x,\bar{y}) = \frac{x}{4\bar{y}}(3\bar{y}^2 + 2\bar{y} - 1)\,, \tag{17}$$

$$K_{1c}(x,\bar{y}) = \frac{1}{2}(\bar{y}^2 + 2\bar{y} - 1)\,, \tag{18}$$

$$K_{2a}(x,\bar{y}) = \frac{1}{2}(2\frac{x}{\bar{y}} - 1)(\bar{y}^2 + 2\bar{y} - 1)\,, \tag{19}$$

$$K_{2b}(x,\bar{y}) = \frac{x}{4\bar{y}}[\bar{y}^2 + 3(2\bar{y} - 1)]\,. \tag{20}$$

The combinatoric partition function $Z_{comb} = (n_x!)^{-1}\prod_{j=1}^{n_x}\nu_j$ is thus

$$Z_{comb} = \frac{1}{n_x!}\prod_{j=1}^{n_x}\Big\{n_0^{(1-y_X^j-y_Y^j)}(n_0 - jx^2)^{x^2}F_{1b}^{-(x/y_X^j+x/y_Y^j-2)(y_X^j+y_Y^j-1)} \times F_{1c}^{-(y_X^j-x)(y_Y^j-x)}F_{2b}^{-(x/y_X^j+x/y_Y^j-2)(y_X^j-1)(y_Y^j-1)}F_{2a}^{-(y_X^j-1)(y_Y^j-1)}\Big\}\,, \tag{21}$$

where $F_i = n_0 + jM_i$, $M_i = -x^2 + K_i(x,\bar{y})$, and y_X^j and y_Y^j are the disorder indices of the jth disk.

We note at this point that, as is the case for the combinatoric partition function for long hard rods [5], concentration dependencies of second and higher order do not appear in Eq. (21), which is an inherent feature of the commonly used Onsager [4,42] and Flory approaches. This approximation, as already pointed out by Onsager [4], can be justified for long hard rods, but requires careful evaluation when applied to disks, as was shown by a Monte Carlo study of a system of thin hard disks [39].

In order to manipulate Z_{comb} into a more tractable form we note that the right-hand side (RHS) of Eq. (21) is dominated by factors quadratic in x. Lower order terms in x are merely correction terms. Furthermore, the dominant factors can be written in the form $(\alpha + \beta j)^\beta$, while the remaining terms, exclusive of the first term $n_0^{(1-y_X^j-y_Y^j)}$, are of the form $(\alpha + \beta j)^\gamma$, where β and γ are, in general, j dependent, i.e., varying from disk to disk within the system, cf. Eq. (21).

Consequently, the following approximations can be applied:

$$\prod_j^{n_x}(\alpha + \beta j)^\beta \approx \prod_j^{n_x}\frac{[\alpha + \beta(j+1)]!}{(\alpha + \beta j)!} = (\alpha + \beta n_x)!\,, \tag{22}$$

and

$$\prod_j^{n_x}(\alpha + \beta j)^\gamma = \left\{\prod_j^{n_x}(\alpha + \beta j)\right\}^\gamma = \left\{\beta^{n_x}\frac{(\alpha/\beta + n_x)!}{(\alpha/\beta)!}\right\}^\gamma\,. \tag{23}$$

The approximation of Eq. (22) is not severe, because the j dependence of β is preserved. The approximation of Eq. (23) referring to a simplified system of "average" disks (γ independent of j) is more severe, but since it is applied to the less important correction terms its use is allowable.

The dominant factors in Eq. (21) are $(n_0 - jx^2)^{x^2}$ and $F_{1c}^{M_{1c}}$; the latter is isolated from $F_{1c}^{-(y_X^j-x)(y_Y^j-x)}$ by rearranging exponents, viz.,

$$F_{1c}^{-(y_X^j-x)(y_Y^j-x)} = F_{1c}^{M_{1c}}F_{1c}^{x(y_X^j+y_Y^j)-y_X^jy_Y^j-K_{1c}(x,\bar{y})}\,. \tag{24}$$

Upon applying Eq. (7) and Eqs. (22)–(24) to Eq. (21), followed by introduction of Stirling's approximations for the factorials, the "steric" partition function becomes

$$-\ln Z_{comb} = 2n_x(\bar{y} - 1) + n_s\ln v_s + n_x\ln(v_x/x^2) + n_0(\bar{y} - 1)^2M_{2a}^{-1}Q_{2a}\ln Q_{2a} + n_0(\bar{y} - x)^2M_{1c}^{-1}Q_{1c}\ln Q_{1c} + n_0(2x/\bar{y} - 1)[(\bar{y} - 1)^2M_{2b}^{-1}Q_{2b}\ln Q_{2b} + (2\bar{y} - 1)M_{1b}^{-1}Q_{1b}\ln Q_{1b}]\,, \tag{25}$$

where

$$Q_i = 1 + \frac{n_x}{n_0}M_i\,, \tag{26}$$

and $v_s = n_s/n_0$ and $v_x = n_x x^2/n_0$ denote the volume concentrations of solute and solvent, respectively.

2. *Orientational factor Z_{or}*

The orientational part of the partition function is approximated in exactly the same way as Flory has done for rods [5], viz.

$$Z_{or} = \frac{n_x!}{\prod_k (n_{xk})!} , \tag{27}$$

where n_{xk} denotes the number of disks whose symmetry axis orientations occur within the element of solid angle $\delta\omega_k$. To relate Z_{or} to the disk disorder parameter, we assume that the orientational distribution function of the disk symmetry axis, $f(\psi)$, is uniform over solid angle out to some angle ψ_0 and zero beyond, where ψ is the angle between the symmetry axis and the director. Z_{or} is then proportional to ω^{n_x} where ω is the solid angle within $\psi\langle\psi_0$. For small angles ω is to a good approximation proportional to $\langle\sin\psi\rangle^2$, where the notation $\langle\,\rangle$ indicates averaging over the allowed orientations. As ω increases, the approximation is less good [5].

For rods $\langle\sin\psi\rangle$ is simply equal to the average disorder index. To find the relationship between $\langle\sin\psi\rangle$ and $\bar{y}$ for disks we proceed as follows. Let $\sin\psi = H(y)$, such that for a perfectly ordered molecule we have $H(1) = 0$ ($\sin\psi = 0$; $y = 1$, cf. Fig. 1). For small disorder angles ($\psi \cong 0 \Rightarrow y \cong 1$), which is the case of greatest significance in the nematic phase, we can write

$$\sin\psi \cong h(y-1), \quad h = \left.\frac{dH}{dy}\right|_{y=1} . \tag{28}$$

Although the proportionality constant h is of no importance for further calculations [5,14], it can be estimated if one makes the plausible assumption that all disks with the same average disorder index are equivalent. A model disk can be thought of as being made up of either of two mutually perpendicular sets of x rods of length x, one of the sets declined with respect to the **X** axis, and the other with respect to the **Y** axis. By using a relationship between $\sin\psi$ and the disorder index for rods [47,24] and averaging it over the two basic declinations of the disk, we get, cf. Eq. (5),

$$\sin\psi = \left(\frac{y_X - 1}{x} + \frac{y_Y - 1}{x}\right) \Big/ 2 = \frac{y-1}{x} , \tag{29}$$

i.e., $h \equiv x^{-1}$.

The orientational partition function for the nematic phase becomes, therefore,

$$-\ln(Z_{or}) \sim -\ln(\omega^{n_x}) \simeq -2n_x \ln(\bar{y} - 1) . \tag{30}$$

B. Isotropic phase

Our approximate treatment of the combinatory partition function is relevant for a highly ordered system, i.e., for which $\bar{y}/x \ll 1$. Despite this fact we would like to extend the use of Eq. (25) to a completely disordered system as was done routinely by Flory and co-workers [5,14]. The main problems are the form of the orientational part of the partition function and an appropriate definition of the disorder index for the isotropic phase.

Flory's early work on solutions of rods [5] showed that the nematic configurational partition function reduces to that for a randomly disordered polymer solution when $\bar{y}$ is equal to x [48]. Obviously, this argument is inadequate for disks.

A more rigorous argument that $\bar{y} = x$ is a sufficient condition for the nematic phase partition function to be the partition function of the isotropic phase as well was given for rods by Flory and Ronca [14] and Warner and Flory [15]. Since the arguments of Warner and Flory are quite general [15], we employ their approach to evaluate the configurational partition function ($Z_{iso} = Z_{comb} Z_{or}$) and the random disorder value of $\bar{y}_{iso}$ for disks in the isotropic phase.

First, one intuitively expects that, just as for rods, random disorder for disks is described by $\bar{y}_{iso} = x$. Next, if one adopts the considerations which led us to the relation between the disk disorder index and $\sin\psi$, Eq. (29), one can also stipulate that for randomly disordered disks

$$\bar{y}_X = \bar{y}_Y = \bar{y}_{iso} = x . \tag{31}$$

One must keep in mind, however, that the definition of the average disk disorder in Eq. (6) is only valid for low disk disorder, i.e., the solid angle of a pyramid circumscribed by the symmetry axes of the equivalent "square" disks is very close to the solid angle of a cone circumscribed by the symmetry axes of the corresponding physical disklike molecules. With increasing disorder, however, the discrepancy between the two solid angles increases, and the expression for the average disorder index as a function of the declination angle given by Eq. (29) becomes less and less accurate. The intuitively acceptable condition $\bar{y}_{iso} = x$ for the isotropic phase must therefore be verified to see if it does indeed minimize the free energy of mixing.

Following Warner and Flory we write Z_{or} as [15]

$$Z_{or} = \frac{n_x!}{\prod_y [(\omega_y)^{n_{xy}}\, n_{xy}!]} = \prod_y \left\{\frac{\sigma\omega_y n_x}{n_{xy}}\right\}^{n_{xy}} , \tag{32}$$

where n_{xy} denotes the number of molecules with the same y, ω_y is an *a priori* probability of finding a molecule with the chosen y, and σ is an unimportant normalization factor [14].

Note that Eq. (32) is more general than Eq. (27), i.e., it does not require the simplifying assumption of a uniform orientational distribution of disk symmetry axes over a cone $\psi \leq \psi_0$. Instead, cylindrical symmetry of the distribution about the **Z** axis is stipulated, so that a given y describes all molecules inclined by ψ from **Z**. Detailed calculations of the critical parameters for the formation of the nematic phase showed that the critical concentration and the axial ratio calculated with the aid of Eq. (27) and of Eq. (32), respectively, differ by less than 7%, while the difference in the disorder index is slightly higher but nevertheless never exceeds 10% [6,14]. Because of the numerous simplifications already introduced in the course of the combinatory partition function evaluation, especially the K_i functions, we find the use of Eq. (32) in the nematic phase to be an unnecessary complication. It can

TABLE I. Numerical solutions of Eq. (36).

x	$\bar{y}_{iso}$	
	$v_x = 0.01$	$v_x = 0.99$
4.0	4.01	4.06
6.0	6.32	6.34
8.0	8.74	8.76
10.0	11.27	11.23
12.0	13.89	13.82

be used, however, to advantage in the isotropic phase.

The configurational partition function ($Z = Z_{comb}Z_{or}$) can in general be written down with the aid of Eq. (3), Eq. (32), and the Stirling approximation as follows:

$$-\ln Z = -\ln Z_{comb} + \sum_y n_{xy} \ln\left(\frac{n_x \omega_y}{n_{xy}}\right) - n_x \ln(\sigma) \ . \tag{33}$$

The orientational equilibrium distribution function (n_{xy}/n_x) can be found from the usual condition [15]

$$\frac{\partial(-\ln Z)}{\partial n_{xy}} = 0 \ , \tag{34}$$

a general solution of which can be written as [14]

$$\frac{n_{xy}}{n_x} = f_1^{-1} \omega_y \exp[-A(x,\bar{y})y] \ , \tag{35}$$

where f_1 is a normalization factor. Since in the isotropic phase the orientational distribution is uniform over all angles, $A(x,\bar{y})$ in Eq. (35) should be equal to zero [14]:

$$A(x,\bar{y}) = 0 \ . \tag{36}$$

In the case of disks, Eq. (36) cannot be solved analytically. Substituting the expression for Z_{comb}, Eq. (25), into Eq. (33), and solving Eq. (36) numerically, we find that the equilibrium value of y_{iso} is always somewhat larger than x, and does not depend essentially on the volume concentration of disks, cf. Table I. For small values of x, the difference between the two is very small. With increasing x, the difference increases slightly, e.g., even for $x = 12$, the discrepancy between the two is only about 15%.

The absolute values of the chemical potentials for the isotropic phase depend on the value assigned to $\bar{y}$ in the limit of complete disorder. The use of $\bar{y}_{iso} = x$ instead of the exact value from the solution of Eq. (36), cf. Table I, causes an insignificant variation in $(\mu_x - \mu_x^0)^I$ and in $(\mu_s - \mu_s^0)^I$. Thus changes in the equilibrium compositions are also insignificant. In order to avoid tedious numerical calculations, and to preserve a tractable form of the formalism, we can safely use $\bar{y}_{iso} = x$ and Eq. (31) in subsequent work.

C. Solute-solvent interactions Z_{int}

We would also like to investigate the effect of small interactions between solute and solvent molecules. We assume that the intermolecular forces are sufficiently weak that they do not seriously disturb the assumed randomness for a specified degree of orientation. Consequently, we restrict our considerations to nearest neighbor interactions, i.e., only between those molecules in direct contact with each other. In the Flory lattice method this corresponds to considering interactions between particles which have a common wall between their constituent cells.

Let N_{ij} and ϵ_{ij}, $i,j = x,s$, be, respectively, the number of common walls and the energy of interaction between solvent s and solute x unit cells. The total interaction energy associated with the solvent-solute mixing can then be written as

$$\Delta E = N_{sx}[\epsilon_{sx} - (\epsilon_{xx} - \epsilon_{ss})/2] = N_{sx}\Delta\epsilon \ . \tag{37}$$

The solvent-solute common walls number N_{sx} can be expressed in terms of the volume concentrations of the solvent and solute. The number of disk walls accessible to other particles is

$$2N_{xx} + N_{sx} = 2x(x+2)n_x \ . \tag{38}$$

On the other hand, assuming that N_{xx} is proportional to the disk volume concentration we have

$$N_{xx} \simeq x(x+2)n_x v_x \ . \tag{39}$$

Combining Eq. (37), Eq. (38), and Eq. (39) with the definition $v_x = n_x x^2/n_0$ yields

$$\Delta E = N_{sx}\Delta\epsilon = 2\Delta\epsilon \frac{x+2}{x} n_0(1-v_x)v_x = RT\chi(x)n_s v_x \ , \tag{40}$$

which is the well known van Laar form of the heat of mixing, where $RT\chi(x)$ can be identified as the energy change per cell on transferring a solute molecule from the pure solute to the infinitely dilute solution. Since the $\chi(x)$ dependence on x is weak and for large x can be assumed to be independent of the molecular size, we consider it to be a constant for simplicity, i.e., we adopt the thin disk approximation.

The relevant part of the partition function is thus

$$Z_{int} = \exp(-\Xi v_x v_s) \ , \tag{41}$$

where $\Xi = \chi n_0$ is a temperature dependent scaling factor [16,49].

Combining Eq. (3) and Eq. (41) we may finally write down an expression for the Gibbs potential, cf. Eq. (2).

D. Phase equilibria conditions

The conditions for *NI* biphasic equilibrium are stipulated by the simultaneous equality of the chemical potentials of the same component in both phases, Eq. (1). At the same time there must be orientational equilibrium of the disks in the nematic phase, which requires [5]

$$\frac{\partial G}{\partial \bar{y}} = 0 \tag{42}$$

with $\partial^2 G/\partial \bar{y}^2 > 0$ as a subsidiary condition. The solution of Eq. (42) gives the equilibrium value of $\bar{y}$ for the nematic phase. Since the coexistence of two different nematic phases has been predicted [15,50] and observed [50] for solutions of rods, we also look for possible roots of the NN' biphasic equilibrium equations

$$(\mu_i - \mu_i^0)^N = (\mu_i - \mu_i^0)^{N'} , \tag{43}$$

$$\frac{\partial G^N}{\partial \bar{y}} = 0, \quad \frac{\partial G^{N'}}{\partial \bar{y}'} = 0 , \tag{44}$$

where $i = s$ or x denotes solvent or solute, respectively. It remains to solve numerically the set of equations for the various cases of interest.

III. CALCULATIONS

A. Athermal solutions

Calculations are carried out for x varying in the experimentally interesting range from 2.5 to 14 [30,31]. Numerical solutions of the phase equilibria equations Eq. (1) and Eq. (42) in the absence of solute-solvent interactions ($\Xi = 0$ i.e., athermal solutions) and various values of the molecular volume $v = x^2$ yield the results summarized in Fig. 6 and Fig. 7.

Unfortunately, we are not able to calculate analytically the minimum disk size for absolute stability of anisotropy in the pure solute, x_{cr}. This can only be done numerically.

It is important to note that one of the unphysical consequences that results from the assumption of rectangularly shaped particles is that they can be packed more tightly than round particles. The model, in fact, gives results for which the particle volume fractions approach unity. Although the density scale is clearly off in this limit, these results still form a successful qualitative representation of the high density behavior to the extent that they are interpreted as corresponding to the close-packing limit that occurs at lower volume fraction for rounded particles.

Thus, by setting the disk volume fractions $v_x^* = v_x^{**} \simeq 1$, where v_x^* and v_x^{**} are, respectively, the lower and upper boundary of the biphasic range, and searching for the appearance of a minimum in the free energy with respect to $\bar{y}/x$, one finds the critical size of the disk. As an example, the Gibbs free energy vs $\bar{y}/x$ for several values of x below and above x_{cr} is shown in Fig. 8. We find the minimum critical value of $x_{cr} \simeq 3.015$ (i.e., $v_{cr} \simeq 9.09$) for the coexistence of two phases in the neat system of disks. For $x > x_{cr}$ there always exists some minimum volume concentration of disks v_x^* above which the orientationally ordered phase of the volume concentration v_x^{**} can exist, i.e., there is a minimum of the Gibbs function in $\bar{y}$, $0 < \bar{y} < x$.

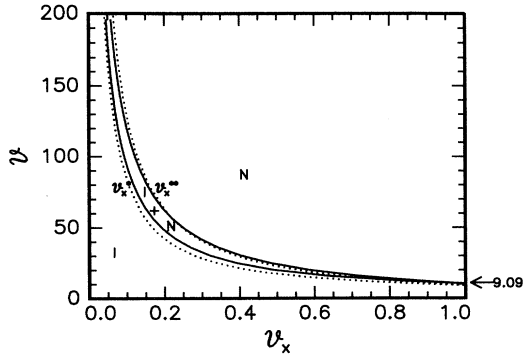

FIG. 6. Athermal mixtures of disks: volume concentrations of phases in equilibrium, v_x, in relation to the molecular volume v (solid lines). I and N denote the isotropic and nematic phases, respectively. Critical concentrations v_x^* and v_x^{**} set boundaries of the coexistence range $I + N$. For comparison threshold concentrations are shown for rods in solution (dotted curves).

For $x > x_{cr}$ between the isotropic and nematic phases there is a range of concentrations (v_x^*, v_x^{**}) where both phases coexist. The concentrations of both phases are constant across the range and equal to v_x^* and v_x^{**}, respectively; the overall concentration of the solution is defined by the volume fraction of conjugated phases, cf. Fig. 6.

With increasing v, the concentrations of both phases decrease substantially, cf. Fig. 6. The concentration of the nematic phase is never much greater than that of the isotropic phase, although the difference increases with initial increase of x above x_{cr}; the v_x^{**}/v_x^* ratio appears to approach 1.3 for $x \approx 8.6$ as the upper limit. At large x we found that both v_x^* and v_x^{**} are inversely proportional to the disk volume, $v_x^* \simeq 9/v$ and $v_x^{**} \simeq 11.5/v$, cf. Fig. 8.

In the nematic phase the nematic order parameter S decrease monotonically with increasing disk volume, and the rate of decrease decreases with v [51]. This behav-

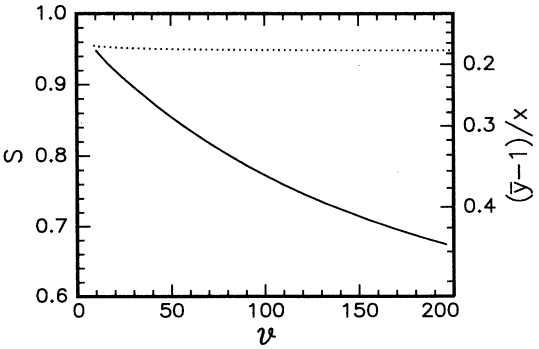

FIG. 7. Athermal mixtures of disks. (LHS) order parameter S and (RHS) normalized disorder index $(\bar{y} - 1)/x$, as a function of molecular volume in the conjugated nematic phase for $v_x = v_x^{**}$. For comparison results are also shown for rods in solution (dotted curve).

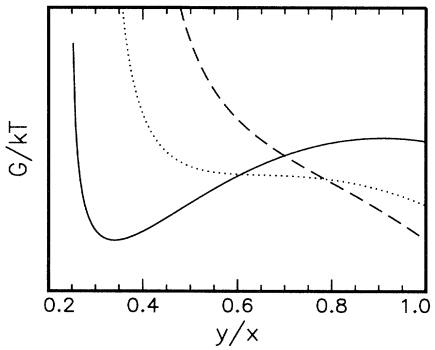

FIG. 8. Athermal mixtures of disks. The nematic phase Gibbs free energy as a function of the normalized disorder index $\bar{y}/x$ is plotted for a few typical values of x, 4 (solid line), 3 (dotted line), and 2.5 (broken line) in the vicinity of x_{cr}. The volume concentration of disks is 0.99.

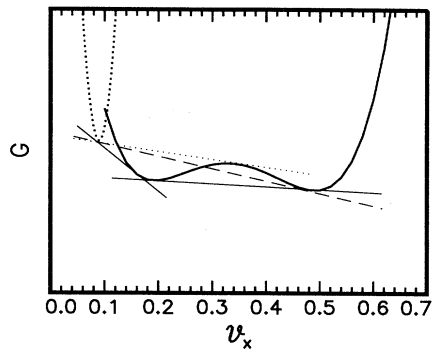

FIG. 9. Nonathermal mixtures of disks. The Gibbs free energy is plotted against volume concentration for (dotted curve) the isotropic and (solid curve) nematic phases for $x = 10$. $\Theta = 0.10$ is characteristic for the coexistence of two nematic phases below the triple point. Common tangency conditions are indicated by common tangent lines: (solid) stable, (broken) metastable, and (dotted) unstable pairs of phases.

ior is essentially different from that observed by Flory for solutions of rods, where orientational order remains fairly constant [5], cf. Fig. 7. For the purpose of comparison, we also carried out phase equilibria numerical calculations for solutions of rods, for the Straley [47] and Romanko and Carr [24] lattice models. A detailed comparison of results for disks and rods will be presented in Sec. IV.

B. Nonathermal solutions

In order to study effects associated with the solvent-solute interactions, we use a reduced inverse temperature $\Theta = \Xi/RT$ rather than the free energy of interaction. We find that a physically plausible range of the inverse temperature is $0 < \Theta < 0.5$, which corresponds to $\infty > T > 50$ K for typical solvent-solute interactions, cf. [52].

Figure 8 shows the utility of plotting the free energy as a function of $\bar{y}/x$ in order to find x_{cr} for the stable orientational order in solution. Similar plots of the free energy vs concentration for different x and Θ facilitated examination of the common tangency condition for phase coexistence. It helped us to clarify the nature of the roots of Eq. (1) and Eqs. (42)–(44), especially the coexistence of more that one pair of phases, cf. Fig. 9.

The numerical results from the concentration-temperature phase equilibria calculations for $x = 8$ and 10 are summarized in Fig. 10. For smaller disks, the isotropic and nematic phases continue to coexist from $\Theta = 0$, which corresponds to the vanishing of soft solvent-solute interactions, through the whole range of inverse temperatures studied. The initially narrow biphasic range $(I + N)$ becomes very wide as the reciprocal temperature is raised, i.e., as the physical temperature is lowered, and this feature is more and more pronounced as x increases. For $x = 8$ indications of more complex behavior for even larger disks are evident. Detailed calculations not included here show that a reentrant feature appears just above the diameter-to-width ratio of about 8.6, and becomes pronounced for $x \geq 9$. The narrow biphasic range $(I+N)$ continues to exist as Θ is raised until a pair of reentrant, concentration dependent, nematic phases appears at a critical inverse temperature Θ_{cr}, cf. Fig. 10 and Fig. 11. At a given inverse temperature, just above the critical point, either of two pairs of phases (I, N) and (N, N') may occur. This situation continues as Θ increases until a triple point at Θ_{III} is reached. The solid lines in Fig. 11 mark the metastable continuations of the phase lines above and below the triple point. For $\Theta \geq \Theta_{III}$, the isotropic phase coexists with the denser and more highly ordered nematic phase N'. This complex phase behavior becomes more and more pronounced, i.e., the difference between Θ_{cr} and Θ_{III} becomes greater and greater, as x increases. We find that the tempera-

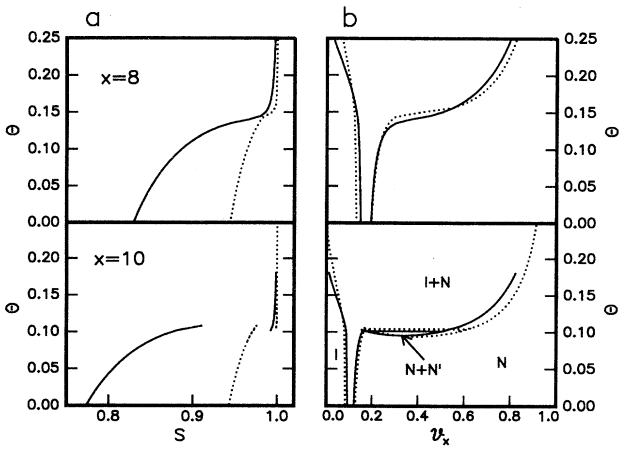

FIG. 10. Nonathermal mixtures of disks. (a) The inverse temperature vs order parameter S, and (b) the inverse temperature-concentration phase diagram for $x = 8$ and 10. Solid lines, disks, and dotted lines, rods with the same molecular volume.

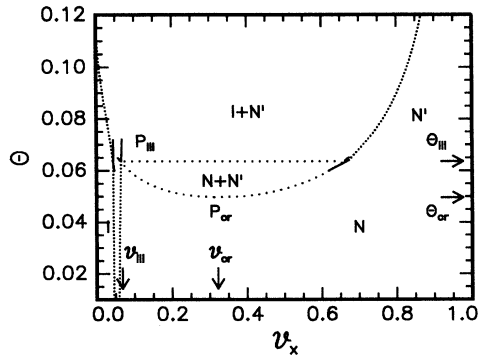

FIG. 11. Nonathermal mixtures of disks. Enlarged phase diagram for $x = 14$ to illustrate the complex phase situation for large disks. The critical P_{cr} and triple P_{III} points with their coordinates are visualized. Metastable coexistence is shown as thin solid lines.

ture and volume concentrations corresponding to the (cr) critical and (III) triple points are roughly linear in the reciprocal disk volume, cf. Fig. 12.

The dependence of the order parameter on inverse temperature for the minimum concentration of the nematic phase v^{**} is also shown in Fig. 10. Lowering the temperature, i.e., increasing Θ, is accompanied by increasing orientational order of the nematic phase. For x below the critical value for the reentrant feature, where there is a rapid broadening of the biphasic range with Θ, the increase of S becomes dramatic, which is the manifestation of a transition from the temperature range where steric effects are dominant to a range where solvent-solute interaction begin to have a significant effect on the formation of the ordered state. When the reentrant phenomenon is present, there is a discontinuity in S (and $\bar{y}$) on going from the less ordered high temperature nematic phase N to the more ordered low temperature nematic phase N'; cf. Fig. 10(a), where the S vs Θ curves overlap over the (N, N') coexistence range.

We show Θ vs S along the bottom boundary of the nematic-nematic coexistence range in Fig. 13. From Θ_{cr}

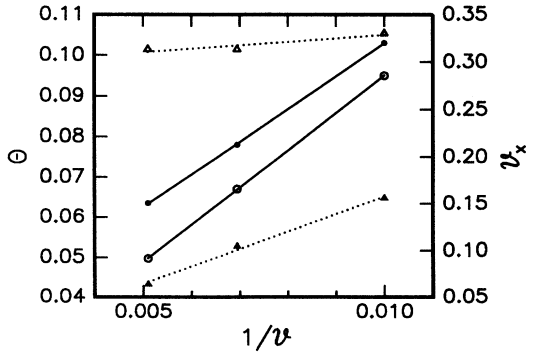

FIG. 12. Nonathermal mixtures of disks. Critical temperatures (θ_{cr}, ○; θ_{III}, •) and concentrations (v_{cr}, △; v_{III}, ▲) vs inverse molecular volume.

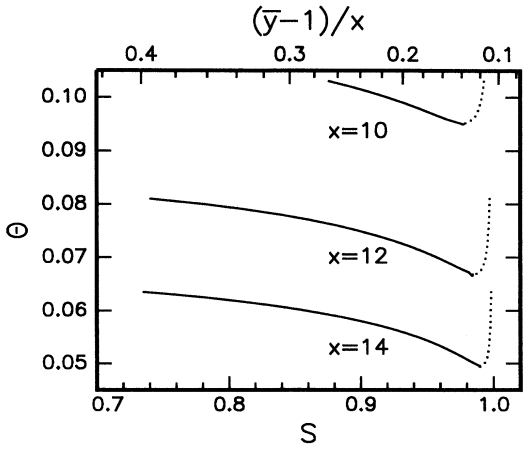

FIG. 13. Nonathermal mixtures of disks. Order parameter S and normalized disorder index $(\bar{y} - 1)/x$ of the two coexisting nematic phases (N-N') as a function of inverse temperature. Dotted lines: more ordered low temperature nematic phase; solid lines: less ordered high temperature nematic phase. For each x lines meet at the critical point.

onwards up to the triple point inverse temperature, the order parameter of the high order nematic phase increases, while that of the low order phase decreases.

IV. DISCUSSION

Experimental data on disklike molecules, macromolecules, or aggregates, which could be relevant for the critical evaluation of our results, are sparse and essentially limited to the lyotropic discotic micelle nematic phase N_D of different two- and multicomponent systems. We will also compare our results, as far as possible, with results of other theoretical work and Monte Carlo simulations.

Perhaps the most interesting feature of the present theory is the prediction of a critical disk size for the formation of a stable nematic phase which coincides nicely with the observed size anisotropy of disklike micelles in the nematic lyotropic phase predicted from other theoretical work. Since the micelle energy is proportional to its surface, the micelle tends to reach the shape of minimum surface (close to a sphere) but anisotropic enough to form the nematic phase. The measured size anisotropy of micelles formed by amphiphilic, lyotropic substances falls in the range from 2.65 to 3.2, depending on the composition and temperature of the lyotropic solution [28,31,53–56], which should be compared with our value of $x_{cr} = 3.015$. Similar conclusions have been reached in previous theoretical work. Y-expansion calculations predicted the threshold value of x for the formation of the nematic phase, $x_{cr} \geq 2.75$ [57]. A similar value was obtained by integral equation methods [58]. Results of Monte Carlo simulations on a system of rodlike and disklike molecules show that a stable N_D phase should exist for $x \geq 2.75$ (hard ellipsoid-of-revolution fluid) [59] or even $x \geq 3$ (hard spherocylinder fluid) [60].

One of the more striking results of this work is the high degree of apparent conformity in the phase diagrams for rods and disks of the same molecular volume. Notably, a symmetry in the thermodynamics of neat systems of either rods or disks has been observed in Monte Carlo simulations [59]. Furthermore, Frenkel and Moulder pointed out that the observed symmetry at low densities is due to the identity of the second virial coefficients for the oblate and prolate ellipsoids of revolution they had been studying. The symmetry in the phase diagram should be expected also at higher densities in those parts of the phase diagram where there is a high degree of orientational order. In light of these findings as well as the relatively low volume fractions and high degree of orientational order predicted by us for the lyotropic N_D, the conformity between the phase diagrams for rods and disks is more than fortuitous.

We found indeed that rods and disks have "equal" anisotropies, i.e., they have equal tendencies to order when their molecular volumes are nearly the same, i.e., a close similarity between phase diagrams for disks and rods is then observed, cf. the dotted lines in Fig. 6 and Fig. 10. In particular, in the athermal limit, i.e., when only steric interactions are present, the stable nematic phase appears only when a certain critical anisotropy is reached, corresponding to almost the same critical molecular volume: 8.75 for rods [24,61] vs 9.1 for disks.

Also, the free energy behavior near the triple point for disks is very similar to that obtained by Warner and Flory for rods [15] which, we believe, reflects a similarity in the assumed solute-solvent interactions for both kinds of solute molecules; compare Fig. 9 here and Fig. 1 of Ref. [15].

A notable but subtle difference can be found, however, in the orientational order parameter dependence on the particle anisotropy. While the order parameter of the discotic nematic phase increases substantially with the disk anisotropy, for rods the order parameter remains almost independent of the anisotropy, cf. Fig. 7 and Ref. [5].

Similar forms of solute-solvent interactions result in very good agreement of the calculated phase diagrams in the biphasic region of two conjugated weakly and strongly oriented nematic phases, where one finds coexistence for nearly identical molecular volumes of rods and corresponding disks. The condition for this coexistence, discussed thoroughly in [50], originates from changes in the chemical potentials induced by soft interactions, which are similar for rods and disks.

We believe that discrepancies between the phase diagrams probably reflect the different degrees of approximation employed in evaluating Z_{comb} for model rods and disks, especially the K_i functions, cf. Eqs. (17)–(20). These differences manifest themselves in a relatively greater divergence between the phase diagrams when the molecular size anisotropy is small and volume concentrations large, i.e., when the lattice method approximations are most suspect, cf. Fig. 6. The two models seem to agree much better for molecular volumes $v > 16$ [62]. Nevertheless, the degree of conformity between the phase diagrams is a confirmation that the approximations and assumptions that enter into our model correspond conceptually to those made in the model for rods.

Finally, we would like to comment on the variation with temperature (and concentration) of the micellar axial ratio and the influence of this effect on the orientational order of micelles in the nematic phase. There is mixed experimental evidence for the temperature dependence of x. In some experiments a relatively constant and well-defined average axial ratio was obtained within the discotic nematic phase. The results of Hendrikx *et al.* [53] indicate a remarkably concentration independent effective shape of the micelle within the entire range of N_D. Also Galerne *et al.* concluded that within the phase the globally averaged effective micellar axial ratio is nearly temperature independent [55]. On the other hand, Boden *et al.* [54] observed that x grows slowly on cooling across the nematic phase temperature range. The variation with temperature of x for the micelles is followed by the variation of the orientational order parameter. Moreover, S increases, on cooling, much faster than the molecular order parameter of thermotropic nematics. The results of Rosenblatt suggest in turn, that the aggregation number of micelles and thus x may be growing with concentration [56].

The results shown in Fig. 10 suggest that the enhancement in the temperature dependence of S may indeed have its origin in the variation with temperature of the micelle diameter. The effect of growth of the diameter of the micelle on cooling is to shift the NI transition to higher temperatures and, consequently, drive the order parameter to larger values.

In summary, the lattice model presented here clearly demonstrates the importance of repulsive interactions in the formation of the nematic phase in discotic systems. In further developments of the model some of the approximations introduced will be eliminated in order to provide us with a better insight into the nature of the isotropic-nematic phase transition in these systems. The model also opens the way to study the formation of the biaxial nematic phase by considering a mixture of rods and disks or anisotropic platelets.

ACKNOWLEDGMENTS

This work was supported by the Scientific Research Committee (Poland), Grants No. 2 0088 91 01 and No. 2 P03B 210 08. Special appreciation goes to Dr. K. Earle for his many helpful suggestions.

APPENDIX

Since an exact evaluation of the occupation factors K_i is cumbersome and the final results are unwieldy, we propose a number of simplifications which yield K_i's that have simple dependencies on $\bar{y}$ and x only, while keeping the error thus introduced in the evaluation of the partition function to a minimum.

First, in order to calculate the mean occupation factor for a particular cell type, say i, we will consider a central cell of type i for which the occupation factor should be a reasonable estimate of K_i, e.g., for cells of type $1b$ or $1b'$ we will consider the middle cell of a particular edge. For cells of type $1c$ or $2c$, we will consider a cell in the middle of the segment. As we shall see, the K_i are second order polynomials in $\bar{y}$; the polynomial coefficients emerge from the analysis. We have verified that p_i is not particularly sensitive to 15% changes in the values of the coefficients. Since we believe that the middle cell factor should be reasonably close to the mean occupation probablility, one may conclude therefore that the proposed estimate will not be a source of significant error in the partition function.

Next, since we assume that the average $\bar{y}$ remains fixed during the process of addition of the solute molecules, it implies that the disorder index of any particular disk, say j, should not significantly differ from the average disorder index of the whole system, i.e.,

$$y_X^j + y_Y^j \cong 2\bar{y}. \tag{A1}$$

The occupation factors are directly related to the numbers of ways N_i^{I} and N_i^{II} in which average molecules [i.e., such that $y_X = y_Y = \bar{y}$, cf. Eq. (12)] built of trains of type I or II, respectively, could block a site to be occupied by the midcell of type i. As it turns out, N_i^{I} and N_i^{II} are directly related to the constituent number of cells in each segment, and to the number of cells of each type in the placing sequence that partitions the segment. We recall that a model disk of given x and disorder indices y_X and y_Y is built up of $y_X y_Y$ segments joined together to form $y_X + y_Y - 1$ trains, each of the trains lying in different neighboring **XY** slices (cf. Figs. 4 and 5). The dimensions of each segment are $(\frac{x}{y_X} \times \frac{x}{y_Y} \times 1)$ which precisely defines the number of unit cells per segment. The segment cells are in turn partitioned into different "kinds" by the placing sequence. For example, the μth segment consists of one cell of μa kind, $(x/y_X - 1)$ cells of μb kind, $(x/y_Y - 1)$ cells of $\mu b'$ kind and $(x/y_X - 1)(x/y_Y - 1)$ cells of μc kind.

Due to the cylindrical symmetry of the nematic phase, we take K_i as the arithmetic mean of N_i^{I}, and N_i^{II}:

$$K_i = \tfrac{1}{2}(N_i^{\mathrm{I}} + N_i^{\mathrm{II}}) \ . \tag{A2}$$

We may now proceed to consider, in turn, each type of cell, always assuming that preceding cells in the sequence are already placed in the **XY** slice, cf. Fig. 5.

1. Occupation factors K_{1b} and $K_{1b'}$

Given the symmetry of the nematic phase, K_{1b} and $K_{1b'}$ are equivalent; thus it is sufficient to consider sites for $1b$ cells only, cf. Eq. (14). All cells up to the midpoint of the $1b$ and $1b'$ edges should already be in place by definition. Now, a site for the next cell of type $1b$ can already be occupied by any cell of type $1b'$ from segments of I-type trains present in the given slice:

$$N_{1b}^{\mathrm{I}} = n_p \frac{x}{y_Y^{\mathrm{I}}} \ , \tag{A3}$$

where y_i^{I} denote the average y_i for I-type trains, $i \equiv X, Y$, and n_p is a number of segments in the I-type train present in the slice. By assumption all **XY** slices are equivalent, so that this procedure takes into account all trains from disks that have already been placed. The contribution from one "average" disk is then:

$$N_{1b}^{\mathrm{I}} = y_Y^{\mathrm{I}} y_X^{\mathrm{I}} \frac{x}{y_Y^{\mathrm{I}}} \quad \text{since} \quad n_p = y_Y^{\mathrm{I}} y_X^{\mathrm{I}}. \tag{A4}$$

In the case of type II trains the situation is different. When the angle between the long axes of the type-II trains and the **X** reference axis is greater then 45°, then their segments are longer along the **Y** axis, i.e., $y_Y < \bar{y}$. The site can then be blocked only by $1b$ cells from their first segments; the fact that $1b'$ cells are already in place from the segment under consideration excludes access to the site by the other segments present in the slice, cf. Fig. 4 and Fig. 5. Thus the contribution from such segments is

$$(y_Y^{\mathrm{II}} + y_X^{\mathrm{II}} - 1) \frac{x}{y_Y^{\mathrm{II}}} \ , \tag{A5}$$

where $(y_Y^{\mathrm{II}} + y_X^{\mathrm{II}} - 1)$ is the number of the first segments, i.e., the number of trains making up an average molecule of type II. For trains of declination angle smaller than 45°, i.e., $y_Y > \bar{y}$, the situation is the same as for type-I trains, cf. Eq. (A4):

$$y_X^{\mathrm{II}} y_Y^{\mathrm{II}} \frac{x}{y_Y^{\mathrm{II}}} \ . \tag{A6}$$

Since we are considering a system of average disks, all possible lengths for a segment side are equally probable, provided that $y_X + y_Y = 2\bar{y}$ =const, the average N_{1b}^{II} is the arithmetic mean of Eq. (A5) and Eq. (A6), and

$$N_{1b}^{\mathrm{II}} = (\bar{y}_Y^{\mathrm{II}} \bar{y}_X^{\mathrm{II}} + \bar{y}_Y^{\mathrm{II}} + \bar{y}_X^{\mathrm{II}} - 1) \frac{x}{2\bar{y}_Y^{\mathrm{II}}} \ . \tag{A7}$$

Combining Eq. (A2), Eq. (A4), and Eq. (A7), and using the cylindrical symmetry of the system, we finally obtain

$$K_{1b}(x, \bar{y}) = K_{1b'}(x, \bar{y}) = \frac{x}{4\bar{y}}(3\bar{y}^2 + 2\bar{y} - 1) \ . \tag{A8}$$

2. Occupation factors K_{1c} and K_{2c}

A careful inspection of Fig. 5 reveals that occupation factors for cells of type $1c$ and $2c$ are the same. We reiterate that $1a$, all of the $1b$ and $1b'$ cells, and a certain number of $1c$ cells are already in place in the slice before we can evaluate K_{1c}. The site for the next $1c$ cell can only be occupied by either the bottom left corner of the type-I trains ($1a$ cells) or by the bottom left corner of any segment of type-II trains.

Consequently,

$$N_{1c}^{\mathrm{II}} = \bar{y}_Y^{\mathrm{II}}\, \bar{y}_X^{\mathrm{II}} \tag{A9}$$

and

$$N_{1c}^{rmI} = \bar{y}_Y^{\mathrm{I}} + \bar{y}_X^{rmI} - 1\ . \tag{A10}$$

With the aid of Eq. (A2) and using Eq. (13) the occupation factors are

$$K_{1c}(x,\bar{y}) = K_{2c}(x,\bar{y}) = \tfrac{1}{2}(\bar{y}^2 + 2\bar{y} - 1)\ . \tag{A11}$$

3. Occupation factor K_{2a}

The first segment of the train is now in place in the slice. The site for the next cell, i.e., the second segment of the first cell, $2a$, can only be occupied by the following types of cells: any of the cells of the $1b$ or $1b'$ edges of segments of type-II trains, or by the same cells of the first segment of type-I trains. Note that access to the site for cells from the other segments of type-I trains is effectively blocked by placing the first segment, cf. Figs. 4 and 5. Therefore

$$N_{2a}^{\mathrm{I}} = (\bar{y}_Y^{\mathrm{I}} + \bar{y}_X^{\mathrm{I}} - 1)\left(\frac{x}{\bar{y}_X^{\mathrm{I}}} + \frac{x}{\bar{y}_Y^{\mathrm{I}}} - 1\right) \tag{A12}$$

and

$$N_{2a}^{\mathrm{II}} = \bar{y}_Y^{\mathrm{II}}\bar{y}_Y^{\mathrm{II}}\left(\frac{x}{\bar{y}_X^{\mathrm{II}}} + \frac{x}{\bar{y}_Y^{\mathrm{II}}} - 1\right)\ , \tag{A13}$$

where $(x/\bar{y}_X + x/\bar{y}_Y - 1)$ is the average number of $1b$ plus $1b'$ cells. Averaging yields

$$K_{2a}(x,\bar{y}) = \tfrac{1}{2}(2x/\bar{y} - 1)(\bar{y}^2 + 2\bar{y} - 1)\ . \tag{A14}$$

4. Occupation factors K_{2b} and $K_{2b'}$

Placing cells of type $2b$ or $2b'$ is similar to placing $1b$ or $1b'$ cells. For type-II trains N_{2b}^{II} is exactly the same as $N_{1b}^{\{\mathrm{II}}$, cf. Fig. 5:

$$N_{2b}^{\mathrm{II}} \equiv N_{1b}^{\mathrm{II}} = (\bar{y}_Y^{\mathrm{II}} + \bar{y}_X^{\mathrm{II}} - 1 + \bar{y}_Y^{\mathrm{II}}\bar{y}_X^{\mathrm{II}})\frac{x}{2\bar{y}_Y^{\mathrm{II}}}\ . \tag{A15}$$

However, the presence of the preceding segment in the slice causes restrictions for the cells of type-I trains. Due to the presence of this segment, access to the candidate site by cells of any segment but the first one is excluded. The first segment of a type-I train can occupy the site only with its $1b$ cells, and we have

$$N_{2b}^{\mathrm{I}} = (\bar{y}_Y^{\mathrm{I}} + \bar{y}_X^{\mathrm{I}} - 1)\frac{x}{\bar{y}_Y^{\mathrm{I}}} \tag{A16}$$

and

$$K_{2b}(x,\bar{y}) = \frac{x}{4\bar{y}}[\bar{y}^2 + 3(2\bar{y} - 1)]\ . \tag{A17}$$

Equations (A8), (A11), (A14), and (A17) complete the set of occupation factors for the problem.

[1] H. C. Longuet-Higgins and B. Widom, Mol. Phys. **8**, 549 (1964).
[2] H. Reiss, Adv. Chem. Phys. **9**, 1 (1965).
[3] H. C. Andersen, D. Chandler, and J. D. Weeks, Adv. Chem. Phys. **34**, 105 (1976).
[4] L. Onsager, Ann. N. Y. Acad. Sci. **59**, 627 (1949).
[5] P. J. Flory, Proc. R. Soc. London Ser. A **234**, 73 (1956).
[6] P. J. Flory and G. Ronca, Mol. Cryst. Liq. Cryst. **54**, 311 (1979).
[7] E. A. Di Marzio, J. Chem. Phys. **35**, 658 (1961).
[8] M. A. Cotter and D. E. Martire, Mol. Cryst. Liq. Cryst. **7**, 295 (1969).
[9] M. A. Cotter and D. E. Martire, J. Chem. Phys. **53**, 4500 (1970).
[10] R. Alben, Mol. Cryst. Liq. Cryst. **13**, 193 (1971).
[11] M. A. Cotter, Mol. Cryst. Liq. Cryst. **35**, 33 (1976).
[12] P. J. Flory, Ber. Bunsenges. Phys. Chem. **81**, 886 (1977).
[13] P. J. Flory and A. Abe, Macromolecules **11**, 1119 (1978).
[14] P. J. Flory and G. Ronca, Mol. Cryst. Liq. Cryst. **54**, 289 (1979).
[15] M. Warner and P. J. Flory, J. Chem. Phys. **73**, 6327 (1980).
[16] R. R. Matheson and P. J. Flory, Macromolecules **14**, 954 (1981).
[17] J. K. Moscicki, S. M. Aharoni, and G. Williams, Polymer **22**, 571 (1981).
[18] J. K. Moscicki, G. Williams, and S. M. Aharoni, Macromolecules **15**, 642 (1982).
[19] J. K. Moscicki and G. Williams, J. Polym. Sci. Polym. Phys. Ed. **21**, 197 (1983).
[20] J. K. Moscicki and G. Williams, J. Polym. Sci. Polym. Phys. Ed. **21**, 213 (1983).
[21] J. K. Moscicki, J. Polym. Sci. Polym. Phys. Ed. **23**, 327 (1985).
[22] J. K. Moscicki, Adv. Chem. Phys. **63**, 631 (1985).
[23] M. Ballauff, Macromolecules **19**, 1366 (1986).
[24] W. R. Romanko and S. H. Carr, Macromolecules **21**, 2243 (1988).
[25] M. P. Taylor and J. Herzfeld, J. Phys. Condens. Matter **5**, 2651 (1993).
[26] S. Chandrasekhar, B. Sadashiva, and K. Sureah, Pramana J. Phys. **9**, 471 (1977).
[27] N. Huu Tinh, C. Destrade, and H. Gasparoux, Phys. Lett. **72A**, 251 (1979).
[28] A. Derzhanski and M. D. Mitov, Mol. Cryst. Liq. Cryst. **152**, 393 (1987).
[29] J. Charvolin, in *Phase Transitions in Soft Condensed Matter*, edited by Tormod Riste and David Sherrington (Plenum Press, New York, 1989), pp. 95–111.
[30] S. Chandrasekhar and G. S. Ranganath, Rep. Prog. Phys. **53**, 57 (1990).
[31] N. Boden, J. Clements, K. A. Dawson, K. W. Jolley, and

D. Parker, Phys. Rev. Lett. **66**, 2883 (1991).
[32] A. Ishihara, J. Chem. Phys. **19**, 1142 1951.
[33] W. Maier and A. Saupe, Z. Naturforsch. Teil A **14**, 882 (1959); **15**, 287 (1960).
[34] R. Diebleck and H. N. W. Lekkerkerker, J. Phys. (Paris) Lett. **41**, 351 (1980).
[35] D. A. Jonah, W. Brostow, and M. Hess, Macromolecules **26**, 76 (1993).
[36] C.-S. Shih and R. Alben, J. Chem. Phys. **57**, 3055 (1972).
[37] L. J. Yu and A. Saupe, Phys. Rev. Lett. **45**, 1000 (1980).
[38] G. E. Feldkamp, M. A. Handschy, and N. A. Clark, Phys. Lett. **85A**, 359 (1981).
[39] D. Frenkel and R. Eppenga, Phys. Rev. Lett. **49**, 1089 (1982).
[40] S. Chandrasekhar, Philos. Trans. R. Soc. London A **309**, 93 (1983).
[41] S. Chandrasekhar, K. L. Savithramma, and N. V. Madhusudana, in *Liquid Cystals and Ordered Fluids*, edited by A. C. Griffin and J. F. Johnson (Plenum, New York, 1984), Vol. 4, pp. 299–309.
[42] A. Stroobants and H. N. W. Lekkerkerker, J. Phys. Chem. **88**, 3669 (1984).
[43] D. Ghose, T. R. Bose, M. K. Roy, M. Saha, and C. D. Mokherjee, Mol. Cryst. Liq. Cryst. **154**, 119 (1988).
[44] J. Herzfeld, J. Chem. Phys. **88**, 2776 (1988).
[45] R. Holyst and A. Poniewierski, Mol. Phys. **68**, 381 (1989).
[46] R. Alben, J. Chem. Phys. **59**, 4299 (1973).
[47] J. P. Straley, Mol. Cryst. Liq. Cryst. **22**, 333 (1979).
[48] P. J. Flory, Proc. R. Soc. London Ser. A **234**, 60 (1956).
[49] Y. Aikawa, N. Minami, and M. Sukigara, Mol. Cryst. Liq. Cryst. **70**, 115 (1981).
[50] E. L. Wee and W. C. Miller, in *Materials of The Symposium of the Division of Colloid and Surface Chemistry, Chicago, 1977,* edited by J. R. Katzer (American Chemical Society, Washington, D.C., 1977), Vol. 3, p. 371.
[51] Since we assumed that the orientational distribution function of the disk symmetry axis is uniform over solid angle out to some angle ψ_0 and zero beyond (with respect to the nematic director), $\bar{y}$ can easily be converted into the orientational order parameter S. To facilitate comparison of our results with available data we decided to use the latter in figures and the following discussion.
[52] P. J. Flory, Adv. Polym. Sci. **59**, 1 (1984).
[53] Y. Hendrikx, J. Charvolin, M. Rawiso, L. Liebert, and M. C. Holmes, J. Phys. Chem. **87**, 3992 (1983).
[54] N. Boden, S. A. Corne, M. C. Holmes, P. H. Jackson, D. Parker, and K. W. Jolley, J. Phys. (Paris) **47**, 2135 (1986).
[55] Y. Galerne, A. M. Figueiredo Neto, and L. Liebert, Phys. Rev. A **31**, 4047 (1985).
[56] C. Rosenblatt, J. Phys. (Paris) **47**, 1097 (1986).
[57] B. Tjipto-Margo and G. T. Evans, J. Chem. Phys. **93**, 4254 (1990).
[58] A. Perera, G. N. Patey, and J. J. Weis, J. Chem. Phys. **89**, 6941 (1988).
[59] D. Frenkel and B. M. Mulder, Mol. Phys. **55**, 1171 (1985).
[60] J. A. C. Veerman and D. Frenkel, Phys. Rev. A **41**, 3237 (1990).
[61] M. Warner, Mol. Cryst. Liq. Cryst. **80**, 67 (1982).
[62] M. Ballauff, Mol. Cryst. Liq. Cryst. **168**, 209 (1989).

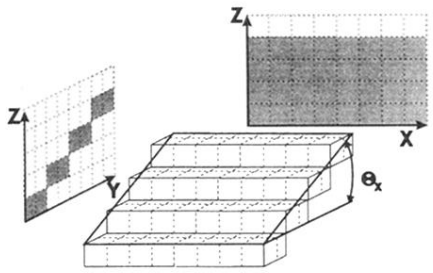

FIG. 2. Disk with $x = 8$ after rotation around the **X** axis by θ_x yelding the disorder index $y_X = 4$. Projections of the disk onto the **XZ** and **YZ** planes are also shown.

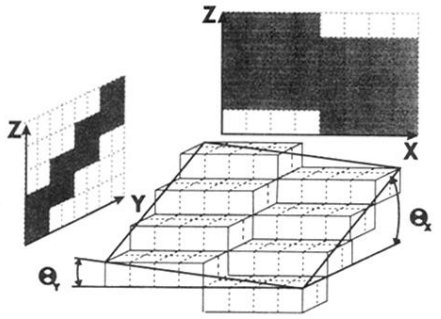

FIG. 3. The same disk after a second rotation around the **Y** axis by Θ_y, $y_Y = 2$.